Theor. Exp. Plant Physiol. (2022) 34:537–550
https://doi.org/10.1007/s40626-022-00263-z

A predictive model of wheat grain yield based on canopy reflectance indices and theoretical definition of yield potential

João Paulo Pennacchi · Nicolas Virlet · João Paulo Rodrigues Alves Delfino Barbosa · Martin A. J. Parry · David Feuerhelm · Malcolm Hawkesford · Elizabete Carmo-Silva

Received: 4 May 2022 / Accepted: 27 September 2022 / Published online: 9 November 2022

Abstract Predicting crop yields through simple methods would be helpful for crop breeding programs and could be deployed at farm level to achieve accurate crop management practices. This research proposes a new method for predicting wheat grain yields throughout the crop growth cycle based on canopy cover (CC) and reflectance indices, named $Yield_p$ Model. The model was evaluated by comparing grain yields with the outputs of the proposed model using phenotypic data collected for a wheat population grown under field conditions for the 2015 and 2016 seasons. Accumulated radiation (RAD), Normalized Difference Vegetation Index (NDVI), Photochemical Reflectance Index (PRI), Water Index (WI), Harvest Index (HI) and CC indices were the components of the model. We found that the biomass accumulation predicted by the model was responsive throughout the crop cycle and the grain yield predicted was correlated to measured grain yield. The model was able to early predict grain yield based on biomass accumulated at anthesis. Evaluation of the model components enabled an improved understanding of the main factors limiting yield formation throughout the crop cycle. The proposed $Yield_p$ Model explores a new concept of yield modelling and can be the starting point for the development of cheap and robust, on-farm, yield prediction during the crop cycle.

Keywords Crop breeding · Early yield prediction · Mathematical modelling · On-farm yield · Remote sensing · *Triticum aestivum*

Supplementary Information The online version contains supplementary material available at https://doi.org/10.1007/s40626-022-00263-z.

J. P. Pennacchi (✉) · J. P. R. A. D. Barbosa
Department of Biology, Federal University of Lavras, Lavras, Brazil
e-mail: jppennacchi@gmail.com

N. Virlet · M. Hawkesford
Sustainable Soils and Crops, Rothamsted Research, Harpenden, UK

M. A. J. Parry · E. Carmo-Silva
Lancaster Environment Centre, Lancaster University, Lancaster, UK

D. Feuerhelm
Syngenta AG, Cambridge, UK

1 Introduction

The increased demand for food motivated by the growing world population (Godfray et al. 2010) and changes in food consumption patterns (Pingali 2006) has increased the pressure on the agricultural sector. Increasing food production in a sustainable way, i.e. with minimal to no increases in land and water and nutrients inputs, emerges as the main solution for ensuring food security in the near future (FAO 2002). Improving yields is the main cornerstone for improving food security, as yield increases are expected to

result in up to 77% of the increases in food production by 2050 (Alexandratos and Bruinsma 2012), while reducing agricultural impacts on the environment (Tilman and Clark 2015). The understanding of the yield formation and the main limitations to this process at the farm level is crucial to the success of breeding programs aiming to improve yield potential and resilience (Reynolds and Langridge 2016).

Yield potential (Yp) is defined as the yield of a cultivar when grown in environments to which it is adapted, with nutrients and water non-limiting, with pests, diseases, weeds, lodging, and other stresses effectively controlled (Evans and Fischer 1999), and is theoretically presented as: $Y_p = RAD \cdot \varepsilon i \cdot \varepsilon c \cdot \varepsilon p$ (Long et al. 2015). The equation represents the energy transformation process from sunlight to grain matter and the efficiencies (ε) involved in this process. The radiative energy from sunlight (RAD) is intercepted by the canopy (εi) and converted (εc) into chemical energy, which is stored in the form of biomass. This biomass is then partitioned (εp) to the organ of interest (e.g. the grain, for the wheat crop) (Monteith and Moss 1977). However, the yield potential is not achieved at the farm level, mainly due to non-ideal growth conditions (Hengsdijk and Langeveld 2009). The difference between the yield potential and the on-farm yield is defined as the yield gap (Lobell et al. 2009).

In the past decades, crop breeding programs focused mostly the increase of yield potential (as discussed by Pennacchi et al. 2018b; Fischer et al. 2014), but future strategies should maintain the efforts to increase the yield potential while decreasing the yield gap (Araus et al. 2008). In breeding programs, the detection of high-yielding cultivars early in the crop cycle improves the capacity of disregarding genetic materials with low yield potential at early stages, focusing on more promising genotypes. (Marti et al. 2007; Prasad et al. 2007; Becker and Schmidhalter 2017). Early yield prediction is also relevant for defining farm practices such as fertilization (Marti et al. 2007) and informing the grain market and insurance companies (Balaghi et al. 2008).

To improve early yield prediction, remote sensing tools such as passive spectro-radiometers have been extensively used. Numerous studies have reported significant correlations between various spectral reflectance indices (SRIs) derived from spectral measurement and wheat grain yield (Raun et al. 2001; Babar et al. 2006; Marti et al. 2007; Balaghi et al. 2008; Peñuelas et al. 2011; Gizaw et al. 2016; Pradhan et al. 2014; Pennacchi et al. 2018a). However, their combinations in a mathematical model are not frequent, despite the mentions in the literature (Raun et al. 2001; Singh et al. 2006; Montesinos-López et al. 2017).

Certain SRIs reflect different canopy characteristics, which means that they can be combined into a single model to fit the equation of theoretical definition of yield (Long et al. 2015). The NDVI (Normalized Difference Vegetation Index) is a vegetation index correlated to area cover by green tissues, and is related to εi. The PRI (Photochemical Reflectance Index) is a pigment-related index correlated to dissipation of excessive radiation and light conversion, and thus related to εc; HI (Harvest Index) is directly related to εp. Finally, WI (Water Index) correlates to the plant water status (Pietragalla et al. 2012). The use of WI in the model includes a term related to the general water status of the canopy and plant vigour. Changes in water availability, and possibly drought and heat stresses, will directly impact on NDVI and PRI. Therefore, adding a component related to canopy water status may turn the model more representative to the potential impact of drought to on-farm yield. Such a model fitting is associated to the high impact of drought in resource use efficiency and crop yield (Davies 2014). This may be true mainly considering the fact that water limitation is one of the key constraints of crop productivity (Dodd et al. 2011), and highly impacts yield (Jin et al. 2016; El-Hendawy et al. 2017).

Empirical models may not be particularly informative if their parameters have no intrinsic biological meaning (Adams et al. 2017). Simplicity and ease of application are also desirable characteristics of yield prediction models (Hoefsloot et al. 2012). Modelling crop yields in a single environment may prove challenging, mainly in conditions where treatment factors are absent. For instance, crop yield modelling for germplasm growing under different nitrogen concentrations or water regimes tends to present higher predictive power, as the additional factors may increase observation number and increase the spread of the data (Hernandez et al. 2015; Montesinos-López et al. 2017). Working with germplasm in a single environment and in the absence of treatments relies solely on genetic variability.

In this study, the efficiency of multiple compositions of yield prediction models based on wheat canopy traits, such as reflectance parameters and CC indices was evaluated and compared to alternative statistical modelling methods. The model proposed was based on the yield formation equation and the underlying processes associated with the three efficiencies, εi, εc and εp (Long et al. 2015), and was applied to a wheat population grown in the field for two seasons. The dataset presented herein is part of a larger dataset already exploited for analysis of wheat yield drivers in the same population (Pennacchi et al. 2018a).

2 Material and methods

2.1 Plant material and field experiments

A wheat population comprised of double-haploid lines (DHL) generated by Syngenta (Cambridge, UK) was used (Pennacchi et al. 2018a). The population was composed by the two parents and 119 lines, grown at the Rothamsted Research farm in Harpenden, UK, for two consecutive season. The first sowing was in October 2014 and harvested in August 2015, and the second in October 2015 and harvested in August 2016. Each experiment was identified by the year of harvest and their details are presented in the sequence.

The 2015 experiment was planted at the Pastures field after oilseed rape crop in a Typical Batcombe soil (Avery and Catt 1995) in 2×1 m (2 m^2) plots of 6 rows, with a sowing rate of 350 seeds m^{-2}, in three randomized blocks (sown on 20/10/2014 and harvested on 23/08/2015). The 2016 experiment was planted at the Delafield field, in a Batcombe soil (Avery and Catt 1995) after oilseed rape crop, in 4×1 m (4 m^2) plots of 6 rows, with a sowing rate of 350 seeds m^{-2}, in three randomized blocks (sown on 12/10/2015 and harvested on 24/08/2016).

Application of fungicides, insecticides and herbicides, as well as fertilizers, followed Rothamsted farm practices.

2.2 Meteorological data

The meteorological data was acquired from the Rothamsted Meteorological Station at the Rothamsted Farm. The distance from the station to the experiments in a straight line was: 1 km for the 2015 experiment and 1.6 km for the 2016 experiment. The daily radiation (MJ m^{-2}) was recorded and the accumulated radiation (RAD) over a specific period was calculated as the sum of the daily value from the first to the last day in the considered period.

2.3 Crop development

The date at which half of the plants in a plot reached a given growth stage was monitored throughout the growing season using the Zadoks scale (Zadoks et al. 1974). The scale is based on scores relative to crop development stages: tillering, stem elongation, booting, flag leaf expansion, ear emergence, flowering, grain filling and maturation. The frequency of crop development monitoring depended on the crop stage, being less frequent when crop development was at early stages (from tillering (Z2) to booting (Z4) stages) and more frequent from booting (Z4) to dough development (Z8) as the crop development was faster. Leaf senescence was measured from anthesis to the end of the season using the wheat senescence scale (Pask and Pietragalla 2012).

2.4 Phenotyping

Measurements were taken over the crop growing season as described below. For CC, horizontal photographs of the canopy from above, parallel to the soil surface of the plot, were taken weekly from March (Z2.4) to August (Senescence score 10, S10) using a digital camera. The pictures were analysed using the BreedPix open access software that outputs the area covered by green tissue as a percentage of the total area, i.e. the CC (Casadesus et al. 2007). From this data, the following indices were calculated (Fig. 1):

Early vigour (EV): based on Rebetzke and Richards (1999) and calculated as the sum of the weekly single measurements of leaf cover from Z2.4 and the date when plots reached an average of 90% of area covered by leaves (90C) (Eq. 1):

$$EV = \left(\sum_{Z2.4}^{90C} \mathrm{CC} \right). \quad (1)$$

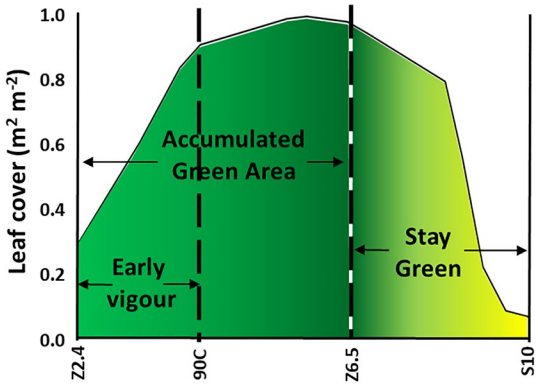

Fig. 1 Graphic representation of leaf cover indices in the experimental wheat field calculated from field level. Leaf cover is given in m^2 of leaf area per m^2 of soil. Early vigour, as accumulated leaf area from Z2.4 to the date when 90% of plot area cover by leaves was reached; Accumulated green area, as accumulated leaf area from Z2.4 to Z6.5; Stay green, as accumulated leaf area from Z6.5 to S10. Z, Zadoks scale for crop development (Zadoks et al. 1974); 90C, 90% of plot area cover by leaves; S, senescence scale (Pask and Pietragalla 2012). Adapted from Pennacchi et al. (2018a). (Color figure online)

Accumulated green area (AGA): calculated as the sum of the weekly single measurements of CC from Z2.4 to Z6.5 (Eq. 2):

$$AGA = \left(\sum_{Z2.4}^{Z6.5} \mathrm{CC}\right). \quad (2)$$

Stay green (SG): based on Thomas and Smart (1993) and calculated as the sum of the weekly single measurements of CC from Z6.5 to S10 (Eq. 3):

$$SG = \left(\sum_{Z6.5}^{S10} \mathrm{CC}\right). \quad (3)$$

Reflectance was measured 75 cm above the canopy using a HandySpec System (TEC5, Oberursel, Germany) spectroradiometer. From the reflectance measurements, the following traits were calculated using the software accompanying the HandySpec System and according to Pietragalla et al. (2012):
Normalized Difference Vegetation Index (NDVI) (Eq. 4):

$$\mathrm{NDVI} = \left(\mathrm{R}_{900} - \mathrm{R}_{680}\right)/\left(\mathrm{R}_{900} + \mathrm{R}_{680}\right). \quad (4)$$

Photochemical Reflectance Index (Eq. 5):

$$\mathrm{PRI} = \left(\mathrm{R}_{530} - \mathrm{R}_{570}\right)/\left(\mathrm{R}_{530} + \mathrm{R}_{570}\right). \quad (5)$$

Water Index (WI) (Eq. 6):

$$\mathrm{WI} = \left(\mathrm{R}_{970}\right)/\left(\mathrm{R}_{900}\right), \quad (6)$$

where R_λ is the reflectance measured at the wavelength λ (nm).

For the 2015 season, reflectance was measured at 3 time points: Z3.4, Z4.5 and Z6.5. For the 2016 season, the measurements were performed at 10 time points: Z3.7, Z5.7, Z6.5, Z7.1, Z7.5, Z7.8, Z7.9, Z9.4, Z9.7 and Z9.9.

The analysis of biomass at the end of the growing was performed at physiological maturity (Z9.9). The tillers in a 50 cm (2015) or 30 cm (2016) row were manually harvested from the third quarter (middle section) of the third row in each of the 6-row plots. The number of tillers and grains, as well as the straw, spike and grain dry mass and grain moisture were measured (Pask and Pietragalla 2012). Harvest index (HI) was calculated as the ratio between dry grain mass (GM) and above ground biomass (AGB, consisting of grain and straw mass), all measured in grams (g) and at 100% dry matter (Eq. 7):

$$\mathrm{HI} = \mathrm{GM}/\mathrm{AGB}. \quad (7)$$

For the final harvest of the experiments, plants were harvested using a Haldrup-C65 (Haldrup, Le Mans, France) plot combine. Grain mass for each plot was determined by the combine. Grain moisture was measured using a sub-sample of grains from each plot at harvest time, and grain mass was normalized to 15% moisture content. Grain mass per plot was corrected for the sections harvested by hand and grain yield estimated in tons per hectare at 85% dry matter.

2.5 Grain yield modelling

Models were fit starting from the simplest and progressing towards increasing complexity with the inclusion of additional traits. The simplest model (Model 1) to predict wheat grain yield included NDVI, PRI and HI. PRI was embedded within the calculation of light use efficiency (LUE) using the conversion factor defined by Wu et al. (2015) (Eq. 8):

$$\mathrm{LUE} = (6.6 \cdot \mathrm{PRI}) + 1.1. \quad (8)$$

Thus, Model 1 was defined as:

$$\text{Biomass}_{M1} = \sum_{i}^{f}(\text{RAD} \cdot \text{NDVI} \cdot \text{LUE}) \quad (9)$$

$$\text{Yield}_{M1} = \text{Biomass}_{M1} \cdot \text{HI}, \quad (10)$$

where Biomass_{M1} is the predicted accumulated biomass, Yield_{M1} is the predicted yield, RAD is the sunlight radiation in the given crop growing period, LUE is the light use efficiency calculated from PRI, and HI is the harvest index; *i* and *f* are initial and final measurement points, respectively.

A second model (Model 2) was built from Model 1 by incorporating a factor related to canopy water. The Water Status index (WS) was calculated as the inverse of WI (Eq. 11). WI is negatively related to canopy water; therefore, higher WI corresponds to lower canopy water content:

$$\text{WS} = \frac{1}{\text{WI}}. \quad (11)$$

The Model 2 was defined as:

$$\text{Biomass}_{M2} = \sum_{i}^{f}(\text{RAD} \cdot \text{NDVI} \cdot \text{LUE} \cdot \text{WS}), \quad (12)$$

$$\text{Yield}_{M2} = \text{Biomass}_{M2} \cdot \text{HI}. \quad (13)$$

A third model (Model 3) was built from Model 1, by using a correction factor for NDVI (NDVI_{cor}). NDVI_{cor} was calculated from NDVI multiplied by a factor related to CC indices (Eq. 14). The correction factor for each line was calculated by the chosen CC index for the line divided by the average of the index for the population. The indices used for each of the periods in the season were: EV from Z3.4 to 90C, AGA from 90C to Z6.5 and SG from Z6.5 to Z9.9 (Fig. 1).

$$\text{NDVI}_{cor} = \text{NDVI} \cdot \text{k}, \quad (14)$$

where *k* is the correction factor defined as (Eq. 15):

$$\text{k} = [(\text{EV}_l/\text{EV}_p)\text{fromZ2.4to90C};(\text{AGAl}/\text{AGAp})\text{from90CtoZ6.5};(\text{SG}_l/\text{SG}_p)\text{fromZ6.5toZ9.9}], \quad (15)$$

where *l* and *p* are, respectively, the line and population mean values for the trait at each time point.

The Model 3 was defined as:

$$\text{Biomass}_{M3} = \sum_{i}^{f}\left(\text{RAD} \cdot \text{NDVI}_{cor} \cdot \text{LUE}\right), \quad (16)$$

$$\text{Yield}_{M3} = \text{Biomass}_{M3} \cdot \text{HI}. \quad (17)$$

The final model (Model 4) was the most complex, resulting from a combination of Models 2 and 3. The Model 4 was defined as:

$$\text{Biomass}_{M4} = \sum_{i}^{f}\left(\text{RAD} \cdot \text{NDVI}_{cor} \cdot \text{LUE} \cdot \text{WS}\right), \quad (18)$$

$$\text{Yield}_{M4} = \text{Biomass}_{M4} \cdot \text{HI}. \quad (19)$$

The Model 4, from here named Yield_p Model, can also be written as:

$$\text{Yield}_p = \left[\sum_{i}^{f}\left(\text{RAD} \cdot \text{NDVI}_{cor} \cdot \text{LUE} \cdot \text{WS}\right)\right] \cdot \text{HI}. \quad (20)$$

As the first measurements were made at stem elongation (Z3.4 for 2015 and Z3.7 for 2016), values for NDVI, PRI and WI were estimated for the early stages when crop growth restarted after winter (around Z2.4). NDVI at Z2.4 was estimated as 35% of the NDVI at Z3.4 (or Z3.7 for 2016) (based on unpublished data collected by the phenotyping group at Rothamsted Research), PRI and WI were estimated as the same values as at Z3.4 (or Z3.7 for 2016). Biomass accumulated at Z2.4 was incipient and considered as zero, being the biomass accumulation counted from this stage. For 2015, the final values for Z9.9 were also estimated, with NDVI as 0.13, LUE as 0.30 and WI as 1.1 (according to average measured values in 2016 season).

The unit of calculation of Yield_p was based on the components of the Eqs. 18 and 19. NDVI_{cor} and WI were measured in percentage and have no unit. RAD was measured in MJ m^{-2} and LUE was measured in g C MJ^{-2} (grams of Carbon per square meter). As HI is also unitless, Biomass and Yield_p are given in g C m^{-2} or converted to t C ha^{-1}.

2.6 Model sensitivity evaluation

Each of the models was evaluated using the Pearson Product Moment (PPM) correlation coefficients (*r*) and the root mean square error (RMSE). The PPM

coefficient represented the correlation between grain yield predicted by each model and measured grain yield. The same approach was used to evaluate the correlation between single traits and measured grain yield. The traits used in the model and the model output (predicted biomass and predicted yield at the end of the season) were compared to measured yield at each of the evaluation time points in 2015 and 2016. The RMSE is defined as the square root of the sum of the squared difference between predicted and measured yield for each observation (line). It was calculated for all the models as:

$$\mathrm{RMSE} = \sqrt{[\sum_{1}^{n}(\mathrm{Yield_p} - \mathrm{Yield_m})^2]}, \quad (21)$$

where n is the number of lines in the experiment (n = 121) and $\mathrm{Yield_m}$ the measured yield for each line.

The use of the two methods of evaluation (PPM and RMSE) results in an integrated and robust analysis of model fitting. The Pearson correlation coefficients (*r*) are related to the model capacity to distinguish the phenotypic response of the cultivars in terms of their grain yield. However, it does not account for the amplitude of the predicted values. The RMSE values accounted for the difference in amplitude between predicted and measured values. An ideal model would present high Pearson correlation coefficient and low RMSE values.

To evaluate the impact of εi, εc and εp in the prediction of yield, each of the terms ($\mathrm{NDVI_{cor}}$, LUE and HI) was individually taken out of $\mathrm{Yield_p}$ Model (Eq. 20) and the output was compared to $\mathrm{Yield_m}$ using PPM correlation coefficient (r) and RMSE. These models are referred as Reduced Models ($\mathrm{Yield_{pR1}}$ to $\mathrm{Yield_{pR3}}$).

To evaluate the impact of increasing the phenotyping frequency, especially after anthesis, a short model was run for 2016 using only the initial predicted time point (Z2.4), three middle time points (Z3.7, Z5.7 and Z6.5) and the last time point (Z9.9). The output was compared to measured grain yield using PPM correlation coefficient (r) and RMSE. This model is referred as Short Model and is only presented for 2016 season.

2.7 Multiple linear regression analysis

A multiple linear regression was independently fit for each of the seasons based in the same traits included in the previous presented model: NDVI, PRI, WI, HI, EV, AGA and SG. Initially, we performed the Forward and Backward Stepwise methods which resulted in a list of parameters to be included in a further model. A final multiple linear regression was fit using a combination of multiple modelling methods (Accumulated, Pooled, Forward Selection, Backward Selection, Forward Stepwise and Backward Stepwise). The final multiple linear regression fitting process was based on fixed and random terms. Fixed terms (terms always present in the model) were the traits which were coincident in both, the Forward and Backward Stepwise methods; random terms (that can be present or absent from the model) were traits which were present in one of the methods but not in the other. Regression fitting was analysed based on the adjusted R-square ($\mathrm{R_{adj}^2}$) and the Mallows Cp coefficient. These models are referred as Multiple Linear Regression (MLR). The GenStat 17th Edition (VSN International Ltd., Hemel Hampstead, UK) was used for all the statistical analysis presented in this paper.

2.8 Data analysis

The method of residual maximum likelihood (REML) was used to evaluate spatial trends over the rows and columns in the field design by fitting a linear mixed model to each measured trait to test for any statistically significant ($p < 0.05$, Chi-squared test) variation. Predicted means from the model fitted to each trait were used in subsequent modelling.

3 Results

3.1 Canopy cover and plant water status indices improve the predictive power of grain yield models

Amongst the four tested approaches to describe the wheat yield from remote sense reflectance indices, from low to high complexity, Model 1 presented a correlation to measured yield of 0.50 and 0.57 for 2015 and 2016, respectively (Table 1). The use of CC corrections to NDVI ($\mathrm{NDVI_{cor}}$) generated an improvement in the fitting of the model from 0.50 ($p < 0.001$) to 0.57 ($p < 0.001$) in 2015 and from 0.57 ($p < 0.001$) to 0.60 ($p < 0.001$) in 2016 (comparison between Model 1 and 3, Table 1). The improvement

Table 1 Evaluation indices for wheat yield prediction models (Model 1 to 4) in relation to measured grain yield, in two years (2015 and 2016)

Models	Model description	2015		2016	
		r	RMSE	r	RMSE
Model 1	$Yield_{M1} = RAD \cdot NDVI \cdot LUE \cdot HI$	0.50	1.66	0.57	0.42
Model 2	$Yield_{M2} = RAD \cdot NDVI \cdot LUE \cdot WS \cdot HI$	0.52	0.97	0.62	1.75
Model 3	$Yield_{M3} = RAD \cdot NDVI_{cor} \cdot LUE \cdot HI$	0.57	1.66	0.60	0.43
$Yield_p$ Model (Model 4)	$Yield_p = RAD \cdot NDVI_{cor} \cdot LUE \cdot WS \cdot HI$	0.59	0.99	0.64	1.75

Significance levels for correlations are given by an F-test on 1 and 120 degrees of freedom: $p < 0.001$. r, Pearson correlation coefficient between predicted and measured yield for each proposed model; RMSE, Root Mean Square Error for each proposed model

$Yield_p$# yield predicted by the proposed Model #, *HI* harvest index, *$NDVI_{cor}$* corrected Normalized Difference Vegetation Index, *LUE* light use efficiency *WS* Water Status index, *RAD* sunlight radiation

was evident in 2015, which suggests that inclusion of the CC indices is most important when reflectance measurements were less frequent.

The use of the WS index (inverse of WI) as an indicator of canopy water status also improved the correlation between predicted and measured yield. For 2015, including WS increased the fitting from 0.50 ($p < 0.001$) to 0.52 ($p < 0.001$), and for 2016 from 0.57 ($p < 0.001$) to 0.62 ($p < 0.001$) (comparison between Model 1 and 2, Table 1).

The combined insertion of both $NDVI_{cor}$ and WS improved the correlation between the predicted and measured yields to 0.59 ($p < 0.001$) in 2015 and to 0.64 ($p < 0.001$) in 2016 (comparison between Model 1 and $Yield_p$ Model, Table 1).

The inclusion of $NDVI_{cor}$ did not change the RMSE as it did not affect the amplitude of the predicted values from Model 1 to Model 3. On the other hand, the inclusion of WS impacted the RMSE as it changed not just the predicted value for each line, but also the general amplitude of the model output. For 2015, the inclusion of WS reduced the amplitude between the predicted and measured values (RMSE from 1.66 to 0.97). For 2016, RMSE changed from 0.42 to 1.75 (Table 1). This contrasting response is associated with the underestimation of predicted yield in 2015 and overestimation in 2016 (Fig. 2). Overall, the $Yield_p$ Model indicated an improved fitting for both years, while it presented an increased RMSE in 2016 (Table 1). The $Yield_p$ Model will be used as the basis for the further analysis presented in the manuscript, unless otherwise stated.

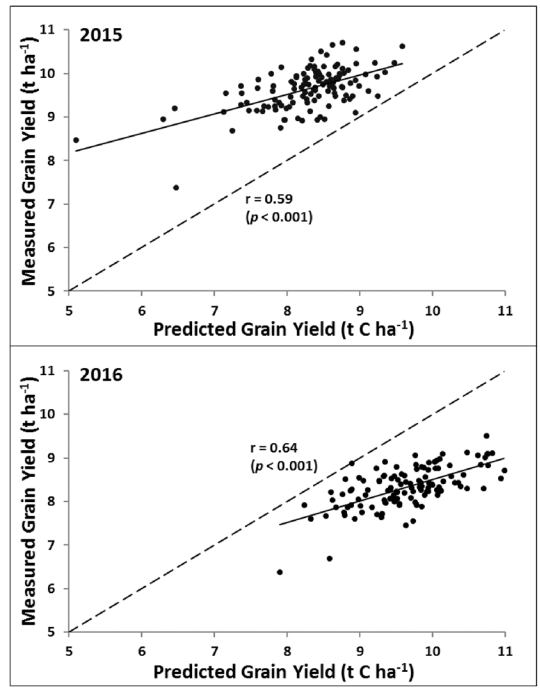

Fig. 2 Yield prediction model for a wheat population grown in the UK in 2015 and 2016. Measured Grain Yield represents grain mass per area determined at full maturity and at 85% dry matter; Predicted Grain Yield represents the output of the proposed $Yield_p$ Model (Eq. 20) based on the yield formation equation. Pearson Product Moment correlation coefficients (r) were calculated to evaluate the correlation between measured and predicted yield at a significance level of 5% (F-tests). Dashed lines represent the 1:1 identity line

3.2 The wheat yield prediction model and grain yield formation

The proposed $Yield_p$ Model presented higher correlation to measured grain yield than any other single trait along the crop cycle in both seasons (Table 2). For the 2015 season, the predicted $Yield_p$ and predicted Biomass presented, respectively, a correlation of 0.59 ($p < 0.001$) and 0.56 ($p < 0.001$), which was higher than the maximum correlations of any measured and/or calculated traits (NDVI (Z3.4), $r = 0.48$, $p < 0.001$; LUE (Z3.4), $r = 0.47$, $p < 0.001$; respectively) (Table 2). For 2016, $Yield_p$ ($r = 0.64$, $p < 0.001$) presented higher correlation to grain yield than the measured and calculated traits, WI (Z7.4) ($r = -0.59$, $p < 0.001$) and LUE (Z3.7 and Z5.7) ($r = 0.44$, $p < 0.001$), respectively (Table 2). The use of the model improved the capacity of predicting yield if compared to single traits by 11% (0.59–0.48 = 0.11) and 5% (0.64–0.59 = 0.05), in 2015 and 2016, respectively.

The correlation between predicted biomass and yield increased along the crop cycle reaching its maximum value around flowering and grain development stages. For 2015, the maximum value was at anthesis (Z6.5; $r = 0.54$, $p < 0.001$), but was also high at booting (Z4.5; $r = 0.53$, $p < 0.001$). For 2016, the maximum correlation was at grain development (Z7.1, Z7.5 and Z7.9; $r = 0.50$, $p < 0.001$) but was close to that at anthesis (Z6.5; $r = 0.48$, $p < 0.001$) and ear emergence (Z5.7; $r = 0.47$, $p < 0.001$) (Table 2).

Table 2 Pearson coefficients (r) for correlation with grain yield for measured and predicted traits (based on the $Yield_p$ Model) in a wheat population grown in the UK in 2015 and 2016

2015		2016		2015		2016	
$Yield_p$	0.59***	$Yield_p$	0.64***	**EV**	0.26**	**EV**	0.30***
HI	0.07^{NS}	*HI*	0.36***	**AGA**	0.42***	**AGA**	0.23**
Biomass	0.56***	*Biomass*	0.48***	**SG**	0.25**	**SG**	0.25**
Biomass (Z3.4)	0.45***	*Biomass (Z3.7)*	0.44***	LUE (*Z3.4*)	0.47***	LUE (*Z3.7*)	0.44***
Biomass (Z4.5)	0.53***	–		LUE (*Z4.5*)	0.42***	–	
–		*Biomass (Z5.7)*	0.47***	–		LUE (*Z5.7*)	0.44***
Biomass (*Z6.5*)	0.54***	*Biomass (Z6.5)*	0.48***	LUE (*Z6.5*)	0.33***	LUE (*Z6.5*)	0.37***
–		*Biomass (Z7.1)*	0.50***	–		LUE (*Z7.1*)	0.37***
–		*Biomass (Z7.5)*	0.50***	–		LUE (*Z7.5*)	0.22*
–		*Biomass (Z7.8)*	0.50***	–		LUE (*Z7.8*)	0.17^{NS}
–		*Biomass (Z7.9)*	0.49***	–		LUE (*Z7.9*)	0.19*
–		*Biomass (Z9.4)*	0.48***	–		LUE (*Z9.4*)	0.01^{NS}
–		*Biomass (Z9.7)*	0.48***	–		LUE (*Z9.7*)	0.01^{NS}
NDVI (*Z3.4*)	0.48***	**NDVI (*Z3.7*)**	0.35***	**WI (*Z3.4*)**	− 0.38***	**WI (*Z3.7*)**	− 0.31***
NDVI (*Z4.5*)	0.28**	–		**WI (*Z4.5*)**	− 0.22*	–	
–		**NDVI (*Z5.7*)**	0.37***	–		**WI (*Z5.7*)**	− 0.22*
NDVI (*Z6.5*)	0.18*	**NDVI (*Z6.5*)**	0.33***	**WI (*Z6.5*)**	− 0.42***	**WI (*Z6.5*)**	− 0.38***
–		**NDVI (*Z7.1*)**	0.40***	–		**WI (*Z7.1*)**	− 0.49***
–		**NDVI (*Z7.5*)**	0.48***	–		**WI (*Z7.5*)**	− 0.55***
–		**NDVI (*Z7.8*)**	0.41***	–		**WI (*Z7.8*)**	− 0.55***
–		**NDVI (*Z7.9*)**	0.41***	–		**WI (*Z7.9*)**	− 0.59***
–		**NDVI (*Z9.4*)**	0.19*	–		**WI (*Z9.4*)**	− 0.32***
–		**NDVI (*Z9.7*)**	-0.08^{NS}	–		**WI (*Z9.7*)**	-0.17^{NS}

Significance levels for correlations are given by an F-test on 1 and 120 degrees of freedom: * $p < 0.05$; ** $p < 0.01$, *** $p < 0.001$, NS not significant. $Yield_p$, yield predicted by the proposed $Yield_p$ Model; HI, harvest index; Biomass, accumulated biomass at the end of the cycle predicted by the $Yield_p$ Model. *EV* early vigour; *AGA*, accumulated green area; *SG*, stay green. Biomass (Z), accumulated biomass at the Z stage predicted by the proposed $Yield_p$ Model. NDVI (Z), Normalized Difference Vegetation Index at the Z stage; LUE (Z), Light Use Efficiency at the Z stage; WI (Z), Water Index at the Z stage. Z is the Zadoks scale value for the plant development stage. Traits in italic were predicted by the model, those underlined were calculated and those in bold, measured

3.3 Sensitivity analysis did not reveal a main influencer for yield prediction

The sensitivity analysis of the $Yield_p$ Model, through the evaluation of the Reduced Models, did not reveal a main influencer for yield prediction. In 2015, the $NDVI_{cor}$ presented the highest influence to the model, followed by LUE and HI. In 2016, HI had a higher influence to yield prediction, followed by $NDVI_{cor}$ and LUE. This lack of a consistent pattern for the influence of individual terms to the final model highlights the flexible response of the model to different seasons (Table 3). Importantly, removing $NDVI_{cor}$ and, especially HI of the model had a large impact on the RMSE value (Table 3), demonstrating that both terms cause a large change in the amplitude of predicted values, which is not observed for LUE. For instance, a HI of 0.5 means that half of the above ground biomass was stored in the grain. A model without HI would generate predicted yield values of an amplitude of the double of the measured value, thus increasing RMSE.

3.4 Increased phenotyping frequency, especially at post-anthesis, improved model fitting

The comparison between $Yield_p$ Model and the Short Model for 2016 allowed an analysis of the impact of the phenotyping frequency in the model fitting, as follow: the $Yield_p$ Model, for 2016, presented a correlation of 0.64 ($p < 0.001$) with a RMSE of 1.75; for the Short model, the correlation was reduced to 0.31 ($p < 0.001$) and the RMSE to 1.54. The increased phenotyping frequency, mainly at post-anthesis, enhanced the fitting of the model for 2016. The improvement of the model fitting promoted by the intensification of phenotyping at post-anthesis cannot be pointed as a general conclusion, as it should be tested for different seasons. The fact that the modelling for 2015, using the same number of time points as the short model for 2016, presented a higher fitting, suggesting the need of evaluating the impact of post-anthesis phenotyping for more years, in repeated experiments.

3.5 The $Yield_p$ model highlights the limitations to yield formation throughout the crop cycle

For the 2016 season, the high frequency of measurements enabled an evaluation of the factors limiting yield formation (Fig. 3). Biomass accumulation was responsive to high NDVI and LUE, until ear emergence (Z5.7). Maintenance of NDVI and an increase in WS, as well as higher solar radiation, kept the biomass accumulation rate until Z7.5, despite a decreased LUE. From Z7.5, biomass accumulation rate decreased with the decrease of NDVI, WS and LUE (Fig. 3).

3.6 Multiple linear regressions were dependent on phenotyping capacity

The use of MLR to predict grain yield using the same traits presented in the $Yield_p$ Model allowed a comparison between the methods, as presented in the sequence. For 2015, the MLR, composed of 7 terms presented $R_{adj}^2 = 37.9\%$ ($r = 0.62$). For 2016, the Multiple Linear Regression composed of 9 terms presented $R_{adj}^2 = 67.3\%$ ($r = 0.82$). Although the MLR presented higher correlations to measured grain yield in both seasons, a high variation in the model fitting

Table 3 Evaluation indices for reduced models from $Yield_p$ model

Reduced models	Model description	2015		2016	
		r	RMSE	r	RMSE
$Yield_p$ Model w/o $NDVI_{cor}$	$Yield_{pR1} = RAD \cdot LUE \cdot WS \cdot HI$	0.49	2.49	0.57	4.89
$Yield_p$ Model w/o LUE	$Yield_{pR2} = RAD \cdot NDVI_{cor} \cdot WS \cdot HI$	0.50	0.50	0.62	1.77
$Yield_p$ Model w/o HI	$Yield_{pR3} = RAD \cdot NDVI_{cor} \cdot LUE \cdot WS$	0.55	7.62	0.48	10.97
$Yield_p$ Model	$Yield_p = RAD \cdot NDVI_{cor} \cdot LUE \cdot WS \cdot HI$	0.59	0.99	0.64	1.75

Significance levels for correlations are given by an F-test on 1 and 120 degrees of freedom: $p < 0.001$. *r* Pearson correlation coefficient between predicted and measured yield for each model, *RMSE* Root Mean Square Error for each proposed model, $Yield_{pR\#}$ yield predicted by the proposed Reduced Model (from 1 to 3), *HI* harvest index, $NDVI_{cor}$ corrected Normalized Difference Vegetation Index, *LUE* light use efficiency, *WS* Water Status index, *RAD* sunlight radiation

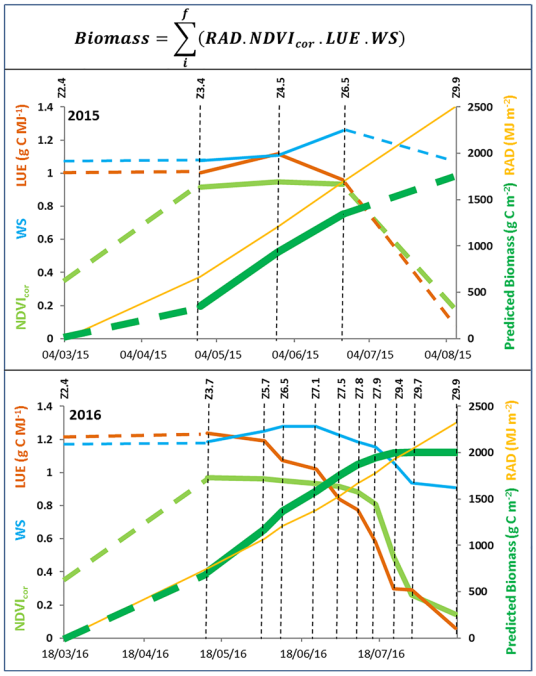

Fig. 3 Graphical representation of the wheat yield prediction model components and their progression during the growing season. Vertical dashed lines represent the measurement time points at specific Zadoks (Z) stages. Coloured dashed lines represent the trendline between estimated and measured points (i.e., before Z3.4/3.7 for both seasons and beyond Z6.5 for 2015). Solid lines represent the connection between measurement points for: LUE (Light Use Efficiency in g C MJ^{-1}; brown), WS (Water Status index, blue), $NDVI_{cor}$ (in %; light green), RAD (Radiation in MJ m^{-2}; yellow) and Predicted biomass (in t C m^{-2}; dark green). (Color figure online)

between 2015 and 2016 was observed. The frequency of phenotyping impacted greatly the reliability of the regressions.

For 2015, the terms presented in the MLR were: AGA, SG, NDVI (estimated at Z2.4), PRI (Z6.5), WI (Z6.5) and HI. For 2016, the terms were: SG, NDVI (estimated at Z2.4, Z9.9), PRI (Z6.5, Z7.4, Z7.8, Z9.9), WI (estimated at Z2.4, Z7.4, Z7.8, Z9.4, Z9.7) and HI. Although some terms contribute to the predictive regressions presented above, they did not present biological meaning, as for instance, canopy WI at the very late stages in the season (Z9.4 and Z9.7), close to harvest. Four terms were presented in the regressions for both years: SG, NDVI (estimated at Z3.4), PRI (Z6.5) and HI. When the linear regression analysis was performed with only these four terms, the final fitting was of $R_{adj}^2 = 30.3\%$ ($r = 0.55$) and $R_{adj}^2 = 41.5\%$ ($r = 0.64$) for 2015 and 2016, respectively. These results were very similar to the general fitting of the $Yield_p$ Model proposed in this article ($r = 0.59$ in 2015 and $r = 0.64$ in 2016) (Table 2).

4 Discussion

The use of a model to calculate wheat grain yield had the main objective of enabling robust predictions of final yield. An additional aim was to unravel the factors contributing for yield formation and the influence of particular combinations of traits measured during the wheat development cycle to the final productivity. Many factors limit biomass accumulation and yield formation during the crop cycle, but they will essentially constrain the efficiencies presented in the yield formation equation. The use of a simplistic model could enhance the understanding of the limitations to yield throughout the crop cycle.

The $Yield_p$ Model, based on the yield formation equation, was developed to predict wheat grain yield using canopy reflectance indices. The model was validated using a wheat population grown and phenotyped under UK field conditions, for two consecutive seasons. The $Yield_p$ Model output presented higher correlation to measured grain yield than any of the single traits measured in the study. Significant correlations between wheat yield and NDVI (Raun et al. 2001; Gizaw et al. 2016; Pennacchi et al. 2018a), PRI (Peñuelas et al. 2011; Gizaw et al. 2016; Pennacchi et al. 2018a) or WI (Pradhan et al. 2014; Pennacchi et al. 2018a) have been previously reported. Here, the mathematical combination of these parameters and CC indices in a simple model has shown an improvement in yield prediction, with correlation coefficients of $r = 0.59$ ($R^2 = 0.35$, $p < 0.001$) and 0.64 ($R^2 = 0.41$, $p < 0.001$) for 2015 and 2016, respectively.

The correlation between predicted and measured yield was intermediate; this may be related to the fact that the models were applied to single environment conditions with the genotypic composition of the lines as the only source of variation. The genetic variability in a double-haploid population is not expected to be as high as in diverse germplasm panels (Gaynor et al. 2017).

The inclusion of CC indices correction to NDVI improved the $Yield_p$ Model fitting, mainly for the

2015 season, when the number of measurements was lower compared to 2016. This method can be useful to improve yield prediction models in field situations where reflectance measurements cannot be frequently performed. It also highlights the importance of using simple tools for obtaining field data (Casadesus et al. 2007) for farmers with limited access to more modern phenotyping equipment. The 2% increase in r when WI was included may seem trivial for this study. However, the effect of including WI in the model may be higher under water deficit. Rather than a canopy water status index, WI is important to account for the stomata control to the diffusive process and used to predict changes in εc (Pietragalla et al. 2012). In combination with NDVI and PRI, WI may also be an indicator of plant vigour and may help to infer about lines with increased resilience to drought and heat stresses, or even impact on the decision of irrigation practices.

The use of WI as part of the model during the whole crop development may be subject to further investigation as, at the later stages of the cycle, a rapid decrease in canopy water status may be favourable to grain maturation and prevention of diseases (AHDB 2016).

One of the strengths of the proposed yield prediction model is the capacity to predict grain yields as early as at the anthesis. In both growing seasons studied, the $Yield_p$ Model predicted biomass accumulated at anthesis (Z6.5) was correlated to measured grain yield. The detection of early predictors of grain yield is a major challenge to plant breeding; the proposed model can decrease the plant selection time, reducing costs and speeding up the release of high yielding cultivars (Becker and Schmidhalter 2017). Anothert contribution of the present study is the capacity to inform the main yield limitation in specific crop stage, which could improve to the understanding of climatic constrains to grain yield. For instance, in 2016, LUE appeared to be the main limitation after ear emergence (Fig. 3), which could be minimized by the maintenance of photosynthetic response from booting to anthesis, as reported by Carmo-Silva et al. (2017).

The comparison of the $Yield_p$ Model with MLR methods allowed to list its advantages and disadvantages, by comparing their specific fittings. Although the MLR methods presented higher correlation to measured yield, they presented different conformations for each of the analysed seasons. The advantage of the $Yield_p$ Model in relation to MLRis is that it responded positively for both seasons with the same conformation, showing its robustness and capacity of application on-farm. The $Yield_p$ Model also estimated yield before the end of the season, being more efficient as a predictive model. The capacity of predicting final yield at early stages in the crop cycle is helpful to inform farmers about crop practices such as late fertilization or crop protection. Contrastingly, MLR methods is recommended for a post-harvest analysis of the main yield drivers in a specific season.

In this study, some factors had to be considered when phenotyping with the aim of yield prediction. NDVI, PRI and WI are influenced by the canopy albedo, which can have diurnal and seasonal variations in wheat (Zhang et al. 2013). SRIs, in general, are affected by external factors as light conditions (overcast), sun position, and also wind. The change in canopy structure caused by the emergence of the ears, as well as its flowers, may have affected the reflectance signal measured. An index like PRI can also present rapid variation according to the light intensity, as well as the air temperature (Gamon et al. 1997; Dobrowski et al. 2005), mainly considering the normal spatial–temporal variation of photosynthesis (Neto et al. 2021). Pennacchi et al. (2018a) also reported high variability for PRI values in the 2015 experiment with the same wheat population. Starting reflectance measurements at early developmental stages, taking measurements at similar weather conditions and time of day, and reducing the time to cover the whole experimental field could potentially improve model fitting by reducing experimental error.

High-throughput methods including phenotyping platforms (Virlet et al. 2017) and unmanned aerial vehicles (UAVs) (Yang et al. 2017) with multi-spectral cameras could improve the data acquisition, the understanding of space–time plant adaption (Galviz et al. 2022) and consequently the model fitting. An increased phenotyping frequency could reduce the influence of each single time point on the final prediction of the model, mainly considering the uncertainty on predicting canopy characteristics in the interval between measurements. The use of SRI calculated from satellite images may be of great advance to yield modelling at field level (Hoefsloot et al. 2012), mainly due to the availability of free-source data as the Landsat database (Wulder et al. 2012). The

adaption of the $Yield_p$ Model to satellite imaging data may allow a further step ahead in yield prediction.

Further improvements to the $Yield_p$ Model could be achieved by the insertion of components that could help explain the main efficiencies involved in the yield formation equation (Long et al. 2015) and the impact of non-ideal growth conditions at the farm level. Moreover, the use of genetic data, related to the traits in the model, could be informative of the genotype-phenotype-environment multiple interactions (Yin and Struik 2010) and improve yield modelling under drought and heat conditions (Parent and Tardieu 2014).

The $Yield_p$ Model was responsive to crop growth and development and capable of predicting biomass and grain yield early in the season with an intermediate fit. Advantages of the proposed model include simplicity, ease of use and low cost of the phenotyping and modelling techniques. Finally, the model presents biological meaning as it is based on the yield formation equation. The application of the model to multiple datasets in different locations and contrasting climatic conditions warrants further study and is likely to reveal new potential for improvement and expanding its practical applications.

Acknowledgements This research was partly supported by the Rothamsted Research Strategic Programs 20:20 Wheat® (BBSRC BB/J00426X/1) and Designing Future Wheat (Biotechnology and Biological Sciences Research Council, BBSRC BB/P016855/1). JPP was funded by the Brazilian CNPq (National Coucil of Research) through the Science without Borders Program for the PhD degree (246221/2012-7). ECS and MAJP acknowledge financial support from the Lancaster Environment Centre. The authors are thankful to the many Rothamsted colleagues and visitors who helped with data collection during field campaign days and sample processing post-harvest. In particular, we would like to thank Mr Andrew Riche for the technical help and Mr Chris Hall for sharing his expertise with sample handling post-harvest. The authors also acknowledge the Rothamsted Farm staff, the Computational and Analytical Sciences department, Rothamsted Research for meteorological data from the e-RA database, which is supported by the UK BBSRC (LTE-NCG BBS/E/C/000J0300) and the Lawes Agricultural Trust.

Author contributions JPP, MAJP, DF and ECS designed research. JPP and ECS performed research. JPP and NV analysed data. JPP, NV, JPRADB, SPL, MAJP, DF and ECS wrote the paper.

Funding This research was partially funded by the BBSRC (Biotechnology and Biological Sciences Research Council), award numbers J00426X/1 and BB/P016855/1, granted to Malcolm Hawkesford.

Declarations

Conflict of interest All authors declare that they have no conflict of interest.

References

Adams MP, Collier CJ, Uthicke S, Ow Y-X, Langlois L, O'Brien KR (2017) Model fit versus biological relevance: evaluating photosynthesis-temperature models for three tropical seagrass species. Sci Rep 7:1–12

AHDB (2016) Wheat disease management guide. Agriculture and Horticulture Development Board, Warwickshire

Alexandratos N, Bruinsma J (2012) World agriculture towards 2030/2050: the 2012 Revision. ESA Working Paper No. 12-03. Agricultural Development Economics Division, Food and Agriculture Organization of the United Nations, Rome

Araus JL, Slafer GA, Royo C, Serret MD (2008) Breeding for yield potential and stress adaptation in cereals. Crit Rev Plant Sci 27:377–412

Avery BW, Catt JA (1995) The soil at Rothamsted, Map prepared by E M Thompson and the Soil Survey and Land Research Centre. Cranfield University, Lawes Agricultural Trust, Harpenden

Babar MA, Reynolds MP, van Ginkel M, Klatt AR, Raun WR, Stone ML (2006) Spectral reflectance indices as a potential indirect selection criteria for wheat yield under irrigation. Crop Sci 46:578–588

Balaghi R, Tychon B, Eerens H, Jlibene M (2008) Empirical regression models using NDVI, rainfall and temperature data for the early prediction of wheat grain yields in Morocco. Int J Appl Earth Obs Geoinf 10:438–452

Becker E, Schmidhalter U (2017) Evaluation of yield and drought using active and passive spectral sensing systems at the reproductive stage in wheat. Front Plant Sci 8:1–15

Carmo-Silva E, Andralojc PJ, Scales JC, Driever SM, Mead A, Lawson T, Raines CA, Parry MAJ (2017) Phenotyping of field-grown wheat in the UK highlights contribution of light response of photosynthesis and flag leaf longevity to grain yield. J Exp Bot 68:3472–3486

Casadesus J, Kaya Y, Bort J, Nachit MM, Arau JL, Amor S, Ferrazzano G, Maalouf F, Maccaferri M, Martos V, Ouabbou H, Villegas D (2007) Using vegetation indices derived from conventional digital cameras as selection criteria for wheat breeding in water-limited environments. Ann Appl Biol 150:227–236

Davies WJ (2014) Exploiting plant drought stress biology to increase resource use efficiency and yield of crops under water scarcity. Theor Exp Plant Physiol 26:1–3

Dobrowski SZ, Pushnik JC, Zarco-Tejada PJ, Ustin SL (2005) Simple reflectance indices track heat and water stress-induced changes in steady-state chlorophyll fluorescence at the canopy scale. Remote Sens Environ 97:403–414

Dodd IC, Whalley WR, Ober ES, Parry MAJ (2011) Genetic and management approaches to boost UK wheat yields by ameliorating water deficits. J Exp Bot 62:5241–5248

El-Hendawy SE, Hassan WM, Al-Suhaibani NA, Schmidhalter U (2017) Spectral assessment of drought tolerance indices and grain yield in advanced spring wheat lines grown under full and limited water irrigation. Agric Water Manag 182:1–12

Evans LT, Fischer RA (1999) Yield potential: its definition, measurement and significance. Crop Sci 39:1544–1551

FAO (2002) The state of food insecurity in the world. ESA Working Paper. FAO, Rome

Fischer RA, Byerlee D, Edmeades GO (2014) Crop yields and global food security: will yield increase continue to feed the world? ACIAR Monograph No. 158, Canberra

Gamon JA, Serrano L, Surfus JS (1997) The photochemical reflectance index: an optical indicator of photosynthetic radiation use efficiency across species, functional types, and nutrient levels. Oecologia 112:492–501

Gaynor RC, Gorjanc G, Bentley AR, Ober ES, Howell P, Jackson R, Mackay IA, Hickey JM (2017) A two-part strategy for using genomic selection to develop inbred lines. Crop Sci 57:2372–2386

Galviz Y, Souza GM, Lüttge U (2022) The biological concept of stress revisited: relations of stress and memory of plants as a matter of space–time. Theor Exp Plant Physiol 34:239–264

Gizaw SA, Garland-Campbell K, Carter AH (2016) Evaluation of agronomic traits and spectral reflectance in Pacific Northwest winter wheat under rain-fed and irrigated conditions. Field Crop Res 196:168–179

Godfray HCJ, Beddington JR, Crute IR, Haddad L, Lawrence D, Muir JF, Pretty J, Robinson S, Thomas SM, Toulmin C (2010) Food security: the challenge of feeding 9 billion people. Science 327:812–818

Hengsdijk H, Langeveld JWA (2009) Yield trends and yield gap analysis of major crops in the world. Wettelijke Onderzoekstaken Natuur & Milieu, Wageningen

Hernandez J, Lobos GA, Matus I, del Pozo A, Silva P, Galleguillos M (2015) Using ridge regression models to estimate grain yield from field spectral data in bread wheat (*Triticum aestivum* L.) grown under three water regimes. Remote Sensing 7:2109–2126

Hoefsloot P, Ines A, van Dam J, Duveiller G, Kayitakire F, Hansen J (2012) Combining crop models and remote sensing for yield-prediction: concepts, applications and challenges for heterogeneous smallholder environments. Publications Office of the European Union, Luxembourg

Jin X, Kumar L, Li Z, Xu X, Yang G, Wang J (2016) Estimation of winter wheat biomass and yield by combining the AquaCrop model and field hyperspectral data. Remote Sensing 8:972–984

Lobell DB, Cassman KG, Field CB (2009) Crop yield gaps: their importance, magnitudes, and causes. Annu Rev Environ Resour 34:179–204

Long SP, Marshall-Colon A, Zhu XG (2015) Meeting the global food demand of the future by engineering crop photosynthesis and yield potential. Cell 161:56–66

Marti J, Bort J, Slafer GA, Araus JL (2007) Can wheat yield be assessed by early measurements of Normalized Difference Vegetation Index? Ann Appl Biol 150:253–257

Monteith JL, Moss CJ (1977) Climate and the efficiency of crop production in Britain. Philos Trans R Soc Lond B 281:277–294

Montesinos-López OA, Montesinos-López A, Crossa J, de los Campos G, Alvarado G, Suchismita M, Rutkoski J, González-Pérez L, Burgueño J (2017) Predicting grain yield using canopy hyperspectral reflectance in wheat breeding data. Plant Methods 13:4–27

Neto MCL, Carvalho FEL, Souza GM, Silveira JAG (2021) Understanding photosynthesis in a spatial–temporal multiscale: the need for a systemic view. Theor Exp Plant Physiol 33:113–124

Parent B, Tardieu F (2014) Can current crop models be used in the phenotyping era for predicting the genetic variability of yield of plants subjected to drought or high temperature? J Exp Bot 65:6179–6189

Pask A, Pietragalla J (2012) Leaf area, green crop area and senescence. In: Physiological breeding II: a field guide to wheat phenotyping. CIMMYT, Mexico, D.F., pp 58–62

Pennacchi JP, Carmo-Silva E, Andralojc PJ, Feuerhelm D, Powers SJ, Parry MAJ (2018a) Dissecting wheat grain yield drivers in a mapping population in the UK. Agronomy 8:94–108

Pennacchi JP, Carmo-Silva E, Andralojc PJ, Lawson T, Allen AM, Raines CA, Parry MAJ (2018b) Stability of wheat grain yields over three field seasons in the UK. Food Energy Security 8:e00147

Peñuelas J, Garbulsky MF, Filella I (2011) Photochemical reflectance index (PRI) and remote sensing of plant CO_2 uptake. New Phytol 191:596–599

Pietragalla J, Mullan D, Mendoza RS (2012) Spectral reflectance. In: Physiological breeding II: a field guide to wheat phenotyping. CIMMYT, Mexico, D.F., pp. 32–36

Pingali PL (2006) Westernization of Asian diets and the transformation of food systems: implications for research and policy. Food Policy 32:281–298

Pradhan S, Bandyopadhyay KK, Sahoo RN, Sehgal VK, Singh R, Gupta VK, Joshi DK (2014) Predicting wheat grain and biomass yield using canopy reflectance of booting stage. J Indian Soc Remote Sensing 42:711–718

Prasad B, Carver BF, Stone ML, Babar MA, Raun WR, Klatt AR (2007) Genetic analysis of indirect selection for winter wheat grain yield using spectral reflectance indices. Crop Sci 47:1416–1425

Raun WR, Johnson GV, Stone ML, Solie JB, Lukina EV, Thomason WE, Schepers JS (2001) In-season prediction of potential grain yield in winter wheat using canopy reflectance. Agron J 93:131–138

Rebetzke GJ, Richards RA (1999) Genetic improvement of early vigour in wheat. Aust J Agric Res 50:291–301

Reynolds M, Langridge P (2016) Physiological breeding. Curr Opin Plant Biol 31:162–171

Singh M, Niwas R, Khichar ML, Yadav MK (2006) Spectral models for estimation of chlorophyll content, growth and yield of wheat crop. J Indian Soc Remote Sensing 34:1–5

Thomas H, Smart CM (1993) Crops that stay green. Ann Appl Biol 123:193–201

Tilman D, Clark M (2015) Food, agriculture & the environment: can we feed the world & save the earth? Am Acad Arts Sci 144:1–23

Virlet N, Sabermanesh K, Sadeghi-Tehran P, Hawkesford MJ (2017) Field Scanalyzer: an automated robotic field phenotyping platform for detailed crop monitoring. Funct Plant Biol 44:143–153

Wu C, Huang W, Yang Q, Xie Q (2015) Improved estimation of light use efficiency by removal of canopy structural effect from the photochemical reflectance index (PRI). Agric Ecosyst Environ 199:333–338

Wulder MA, Masek JD, Cohen WB, Loveland TR, Woodcock CE (2012) Opening the archive: how free data has enabled the science and monitoring promise of Landsat. Remote Sens Environ 122:2–10

Yang G, Liu J, Zhao C, Li Z, Huang W, Yu H, Xu B, Yang X, Zhu D, Zhang X, Zhang R, Feng H, Zhao X, Li Z, Li H, Yang H (2017) Sensing for field-based crop phenotyping: current status and perspectives. Front Plant Sci 8:1–26

Yin X, Struik PC (2010) Modelling the crop: from system dynamics to systems biology. J Exp Bot 61:2171–2183

Zadoks IC, Chang TT, Konzak CF (1974) A decimal code for the growth stages of cereals. Weed Res 14:415–421

Zhang YF, Wang XP, Pan YX, Hu R (2013) Diurnal and seasonal variations of surface albedo in a spring wheat field of arid lands of Northwestern China. Int J Biometeorol 57(1):67–73